



Time Evolution of Cosmic Ray MHD Shocks and Their Emissions

P. P. EDMON¹, T. W. JONES¹, H. KANG².

¹*Department of Astronomy, University of Minnesota, Minneapolis, MN, USA*

²*Department of Earth Sciences, Pusan National University, Pusan 609-735, Korea*

edmonpp@msi.umn.edu

Abstract: We present results of time evolution of oblique MHD plane shocks including diffusive cosmic ray acceleration with backreaction on the plasma flows. The simulations include self-consistent effects of finite Alfvén wave propagation and dissipation. From the computed cosmic ray particle phase space distributions we calculate expected leptonic and hadronic emissions resulting from interactions between the cosmic rays, magnetic fields, the thermal particle population and relevant astrophysical photon fields.

Introduction

Cosmic ray acceleration in strong shocks is highly efficient and naturally leads to substantial modification in the shock structure compared to ordinary gas or MHD shocks described by Rankine-Hugoniot relations. The modified shock compression can greatly exceed that of an adiabatic gas shock and the shock structure includes a foot or precursor where plasma is compressed and heated as it flows against cosmic rays (CRs) streaming ahead of the relatively thin dissipative shock transition. Since the cosmic rays CRs are accelerated by diffusive propagation through the entire shock structure, these shock modifications also alter the spectrum of the CRs compared to the test particle spectrum formed in a discontinuous transition.

The presence of magnetic fields is essential to the physics of diffusive shock acceleration (DSA), because the principal CR scattering mechanism is gyroresonant interaction with Alfvén waves. That is typically modeled by way of the spatial diffusion coefficient for the CRs in an otherwise gasdynamic model of the shock (e.g., [3, 4]). In some calculations the influence of finite streaming of the Alfvén waves with respect to the bulk plasma and the local dissipation of wave energy (i.e., “Alfvén transport”) have been included (e.g., [1, 7, 5]). On the other hand, despite the facts that typically one expects an oblique magnetic field with respect to the shock normal and that the inclusion of significant

Alfvén transport effects imply significant MHD effects, very few calculations have been published that include a full MHD treatment of DSA, especially when the CR spectrum is calculated self-consistently [8, 11]. To explore the importance of such a self-consistent treatment we include all of the above physics in the calculations reported here. Since modified CR shocks are generally evolving structures so long as the CR spectrum continues to extend to higher energies, our treatment is also time dependent.

The CRs accelerated in astrophysical shocks will produce observable electromagnetic emissions through their interactions with the local plasma and ambient radiation fields. The intensity and spectra of these emissions will generally depend on the CR spectrum as well as the structure of the shock. To illustrate the importance of MHD effects in these emissions we include calculations of emissions generated by both leptonic and hadronic CRs in the modified MHD shocks we present here.

Methods and Model Parameters

We carried out our simulations in one spatial dimension, x , using our “Coarse Grained finite Momentum Volume” (CGMV) scheme for solving the CR diffusion-convection equation [9]. The CGMV scheme evolves the first two momentum moments of the CR momentum distribution

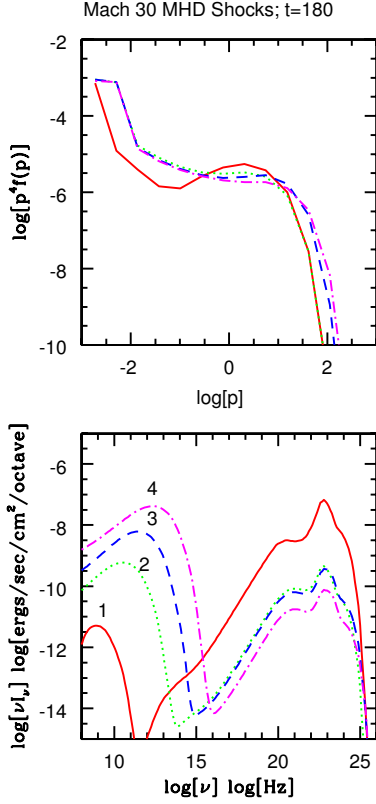


Figure 1: Top: Immediate-postshock CR proton spectra at the gas subshock in four MHD shocks as outlined in the text and in Table 1. Bottom: Intensity of EM emissions from the computed shocks including synchrotron, inverse Compton, bremsstrahlung and secondary pion decays. Numbers correspond to models in Table 1.

function, $f(t, p, x)$, over finite momentum bins, $\Delta \ln p \sim 1$, assuming a piecewise powerlaw momentum dependence for $f(t, p, x)$. The powerlaw slope in each bin is part of the obtained solution. We have demonstrated that this approach provides accurate solutions to the dynamics and the evolution of the CR distribution at greatly reduced computational effort in comparison to finite difference methods. The CGMV routines were incorporated into our well-tested TVD MHD code [6] and CR modified shock solutions were tested against a chain of previously published simulations.

Model	$M_{A,x}$	θ_0	$B_0(\mu G)$	$x_{D,0}(cm)$
1	3000	0	0.46	2.3(14)
2	30	0	46.0	2.3(12)
3	30	30	53.0	2.0(12)
4	30	75	180.0	5.7(11)

Table 1: Shock Model Parameters

We assume upstream of the dissipative subshock that the net scattering turbulence velocity with respect to the plasma is the Alfvén velocity parallel to the local magnetic field vector in response to resonant amplification of upstream-facing Alfvén waves by streaming CRs. Downstream of the subshock we assume isotropic Alfvénic turbulence. We assume also that the Alfvénic turbulence dissipation rate matches the local growth rate produced by resonant scattering; i.e., $-v_A \cdot \nabla P_c = -v_{Ax} \partial P_c / \partial x$ [1]. The simulations include both a dynamically important CR proton and a passive CR electron component. Both components have the same spatial diffusion model; the electrons differ in their evolution only through their energy losses to synchrotron emission and inverse Compton emission of a combined cosmic microwave background and galactic interstellar radiation field. Spatial CR diffusion is isotropic and “Bohm-like”, resulting in an effective diffusion coefficient along the shock normal, $\kappa = \kappa_0 (B_0/B)p$, with $\kappa_0 = (1/3)(m_p c^3 / (e B_0))$. We henceforth express all particle momenta in units of $m_p c$. Subscripts 0 refer to conditions far upstream.

Initially the upstream CR population is void. CR protons and electrons are injected at the subshock following the simple prescription that a fraction ϵ_{inj} of the thermal particle population passing through the shock is injected into the CR population with momenta $p_{inj} = m_p \lambda c_{s,2}$, where $c_{s,2}$ is the post-shock sound speed, and we set $\lambda = 2$. In the simulations presented here the proton injection fraction is $\epsilon_{inj,p} = 10^{-2}$, while the electron value is $\epsilon_{inj,e} = 10^{-4}$.

These shocks all have initial sonic Mach numbers, $M_{s,0} = u_s / c_{S,0} = 30$, with physical shock speed, $u_s = 0.01c = 3000$ km/s. The large scale magnetic field is placed in the $x - y$ plane. We include two parallel shocks ($B_y = 0$, $\theta = \tan^{-1} B_{y,0} / B_x = 0$) with Alfvénic Mach num-

bers, $M_A = u_s/v_{Ax} = 3000$, and 30. There are also two oblique MHD shocks with $M_{Ax} = u_s/v_{Ax} = 30$ and $\theta = 30^\circ$, and 75° . The upstream plasma density, $\rho_0 = m_p n_0 = 1.67 \times 10^{-24} \text{ g/cm}^3$. For a given Alfvénic Mach number this fixes the upstream magnetic field strength, as given in Table 1. Models 2-4 nominally all have the same Alfvén wave advection and dissipation properties.

Results

The properties of the four simulations at $t = 180$ are presented in Figures 1 and 2. By this time each of the shocks is close to reaching its asymptotic postshock compression and pressure values, although the shock transition and the CR spectra would continue to spread self-similarly [9]. The characteristic diffusion length, $x_{D,0} = \kappa_0/u_s$, and diffusion time, $t_{D,0} = \kappa_0/u_s^2$, along with the upstream mass density, ρ_0 provide convenient scaling units. Setting $\kappa_0 = 1$, we have $u_s = 1$ and an upstream gas pressure, $P_{g,0} = 1/1500$. The magnetic field is presented in units such that the magnetic pressure, $P_B = (1/2)B^2$. The full computational box in each case spans the spatial domain $[-100, 100]$, with the associated physical $x_{D,0}$ listed in Table 1.

The four shocks are shown at equivalent times in the sense that test particle DSA theory would predict the same maximum CR momentum, $p_{max} \sim (1/8)t \sim 20$ ($E_{max} \sim 20\text{GeV}$) (e.g., [10]). While that prediction is roughly confirmed in Figure 1, it is also clear that the particle distributions, the predicted emissions and the shock structures show obvious differences among the models. To understand the differences it is easiest to begin with a comparison of the shock structures as illustrated in Figure 2. Here we see that the total shock compression is significantly reduced in all the models with $M_{Ax} = 30$ in comparison to the $M_{Ax} = 3000$ case. That is mostly the result of increased Alfvén wave dissipation in the shock precursor and a reduced net velocity change sensed by CRs across the shock (e.g., [10]). That also leads to a reduced efficiency in CR acceleration, as pointed out by a number of previous authors (e.g., [2]). There is a further reduction in shock compression and

DSA efficiency when the magnetic field is oblique, because the transverse magnetic field component contributes a significant pressure gradient that resists compression through the shock. The total shock compression in the $\theta = 75^\circ$ model 4 is only 1/3 that of the parallel, essentially gasdynamic model 1, and the postshock P_c is reduced by about a factor of two in the same comparison. The particle spectra respond to these trends through a reduction in the concavity below p_{max} , since the reduced compression reduces the spread in velocity changes sensed by particles as they scatter through the precursor. We note for these model parameters and simulation times that the electron and proton CR distributions do not differ substantially.

Although the differences in particle spectra exhibited in Figure 1 are relatively small, they translate into substantial differences in the expected electromagnetic spectra. This is illustrated in the right panel of Figure 1, where we present the intensity of radiation from synchrotron, inverse Compton, bremsstrahlung and secondary pion decay processes found by integrating along a line of sight parallel to the shock normal. The listed order of processes corresponds to the order of dominance in features seen in the intensity plot beginning at low frequencies. The large variation in synchrotron intensity reflects the two orders of magnitude range in magnetic field. More interesting, perhaps, is the large range in the bremsstrahlung and pion decay emissions coming from the large reductions in shock compression and DSA efficiency in the MHD shocks.

Conclusions

MHD CR shocks evolve in noticeably different ways in comparison to gasdynamic CR shocks. Finite Alfvén speeds reduce the efficiency of diffusive shock acceleration. Magnetic pressure gradients through the shock transition reduce compression, further reducing acceleration efficiency. These effects can substantially alter predictions of the nonthermal emissions associated with the shocks, in particular reducing nonthermal X-ray and γ -ray emissions.

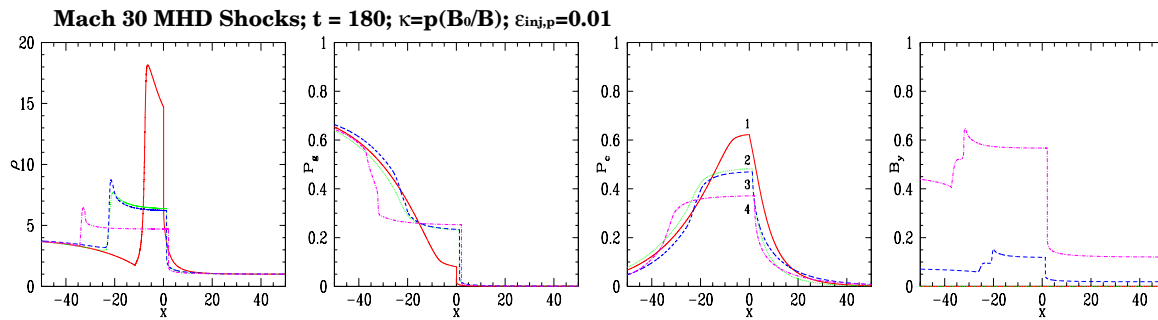


Figure 2: Profiles of the four MHD shocks. Left to right: Gas density, ρ , and pressure, P_g , CR pressure, P_c , and the transverse magnetic field, B_y . Numbers in the P_c plot correspond to models in Table 1.

Acknowledgements

This work is supported at the University of Minnesota by NASA and by the University of Minnesota Supercomputing Institute and at Pusan National University by KOSEF through the Astrophysical Research Center for the Structure and Evolution of the Cosmos (ARCSEC).

References

- [1] A. Achterberg. The ponderomotive force due to cosmic ray generated alfvén waves. *A&A*, 98:195–197, 1981.
- [2] E. Berezhko and H. Völk. Kinetic theory of cosmic rays and gamma rays in supernova remnants. i. uniform interstellar medium. *Aph*, 7:183–202, 1997.
- [3] R. D. Blandford and D. Eichler. Particle acceleration at astrophysical shocks - a theory of cosmic-ray origin. *Phys. Rept.*, 154:1–75, 1987.
- [4] L. Drury. An introduction to the theory of diffusive shock acceleration of energetic particles in tenuous plasmas. *Rep. Prog. Phys.*, 46:973–1027, 1983.
- [5] Ellison D. Berezhko E. and M. Baring. Non-linear shock acceleration and photon emission in supernova remnants. *ApJ*, 540:292–307, 2000.
- [6] A. Frank T. W. Jones and D. Ryu. Time-dependent simulation of oblique mhd cosmic-ray shocks using the two-fluid model. *ApJ*, 441:629–645, 1995.
- [7] T. W. Jones. Alfvén wave transport effects in the time evolution of parallel cosmic-ray-modified shocks. *ApJ*, 413:619–632, 1993.
- [8] T. W. Jones. Time Evolution of Cosmic-Ray Modified MHD Shocks. In *International Cosmic Ray Conference, 29th, Pune, India, August 3-10, 2005 Conference Papers. Volume 3*, pages 269–272, 2005.
- [9] T. W. Jones and H. Kang. An Efficient Numerical Scheme for Simulating Particle Acceleration in Evolving Cosmic-Ray Modified Shocks. *Aph*, 24:75–91, 2005.
- [10] H. Kang and T. W. Jones. Self-similar evolution of cr modified quasi-parallel plane shocks. *Aph*, in press, 2007.
- [11] Morlino G. Blasi P. and M. Vietri. On particle acceleration around shocks. iii. shock waves moving at arbitrary speed. the case of large-scale magnetic field and anisotropic scattering. *ApJ*, 658:1069–1080, 2007.